arXiv:1607.03720v1 [physics.flu-dyn] 13 Jul 2016

The effect of turbulent clustering on particle reactivity

Jonas Krüger[a,*], Nils E. L. Haugen[a,b], Dhrubaditya Mitra[c], Terese Løvås[a]

[a] *EPT, NTNU, Kolbjørn Hejes vei 1B, N-7491 Trondheim, Norway*
[b] *SINTEF Energy Research, N-7465 Trondheim, Norway*
[c] *NORDITA, KTH Royal Institute of Technology and Stockholm University, Roslagstullsbacken 23, SE-10691 Stockholm, Sweden*

Abstract

The effect of turbulence on the heterogeneous (solid-fluid) reactions of solid particles is studied numerically with Direct Numerical Simulations (DNS). A simplified reaction system is used, where the solid-fluid reaction is represented by a single isothermal reaction step. It is found that, due to the clustering of particles by the isotropic turbulence, the overall reaction rate is entirely controlled by the turbulence for large Damköhler numbers. The particle clustering significantly slows down the reaction rate for increasing Damköhler numbers which reaches an asymptotic limit that can be analytically derived. This implies that the effect of turbulence on heterogeneously reacting particles should be included in models that are used in CFD simulations of e.g. char burnout in combustors or gasifiers. Such a model, based on the chemical and turbulent time scales, is here proposed for the heterogeneous reaction rate in the presence of turbulence.

Keywords: Turbulent reacting multiphase flow, char oxidation, clustering

1. Introduction

Particles that are exchanging mass with a surrounding turbulent flow fluid are found in a wide range of situations, both in nature and in industrial applications. Examples of these are pulverized coal combustion in large power plants and fluidized beds in the process industry. A general feature among all these cases is the multi-scale nature of the problem, where the smallest scale is typically the size of the particle, or even the internal structure of the particle, while the largest scale is the much larger size of the entire combustion chamber or reactor. In the intermediate range between these two extremes, one find the scales of the turbulence, which goes from the Kolmogorov scale to the energy carrying scale (the integral scale). Another feature common among these cases is that the particles exchange mass with the surrounding fluid through chemical reactions on the surface of the particles, as e.g. during oxidation or gasification of char.

The effect of turbulence on different large scale properties of the flow, such as turbulent viscosity, diffusivity and conductivity has been known for a long time. A relatively large number of models have been developed in order to account for these effects, such as e.g. the k-ε model [10] and different versions of the Reynolds Stress Models (e.g. [14]). When homogeneous combustion is considered, relatively good models such as the Eddy Dissipation Model [13], different variants of Probability Density Function models (e.g. [7]) or models based on conditioned parameters such as Conditional Moment Closure models (e.g. [11]) are being used. However, for heterogeneous particle reactions, i.e. where the reactions take place at the solid surfaces of the particles, no such model for the effect of turbulence on the chemical reactions has yet been formulated.

A range of efforts to simulate heterogeneous conversion systems under turbulent conditions have been made. Among recent work one can mention that of Silaen and Wang [16] who simulated an existing gasifier with Reynolds-averaged Navier Stokes (RANS) using different turbulence models for the continuum phase and compared their results with measurements. The turbulence effect on particles was included using a stochastic tracking scheme for the particles position, hence turbulence was not taken into account for the heterogeneous reaction rate or transport of gas phase species to the particles. Vascellari et al. [18] ran 2D RANS simulations with kinetics calibrated to experiments and a detailed description of the heterogeneous reactions inside the particle via an effectiveness factor and solving directly for the species partial pressure at the particles surface by assuming local equilibrium. They compare their simulations with measurements from an industrial-scale gasifier and achieve good agreement. Yet, to the knowledge of the authors, only very few studies of combustion or gasification, where account is made for the effect of turbulence on the heterogeneous char conversion, are published, among these are the papers of Luo et al. [12], Brosh & Chakraborty [4] and Brosh et al. [5]. Here,

*Corresponding author
Email address: jonas.kruger@ntnu.no (Jonas Krüger)

the Direct Numerical Simulations (DNS) approach is utilized, where all turbulence scales are explicitly resolved on the computational grid, and hence the effect of the turbulence is implicitly accounted for.

Despite all the effort that has been put into the development of models for turbulent homogeneous combustion or gasification, no good model has been proposed for turbulent heterogeneous combustion or gasification. This means that when particles that experience solid reactions such as during char oxidation (i.e. gas phase species react with the solid part of the particle, not the volatile part) are embedded in a turbulent flow, the turbulence is typically never taken into account in the simulations. The goal of this paper is to highlight the effect of turbulence on solid particles using DNS, and to develop a simple model for the influence of turbulence on reactive particles.

2. Implementation

The direct numerical simulations are performed with the Pencil Code [3], a finite difference code for compressible reactive flows that is fully parallelizable and shows good weak scaling behaviour. It uses a sixth-order finite difference scheme for spatial discretization and a memory-efficient third-order Runge-Kutta scheme [19] for temporal discretization. The particles are treated in a Lagrangian manner and a cloud-in-cell method is used both to interpolate the fluid phase variables at the particles position and for the back reaction from the particles to the fluid.

2.1. Fluid phase equations

In order to isolate the effect of turbulence on reactivity alone, we consider a simplified case with only one reactive species, which is treated as a scalar field advected by the carrier fluid. This reactant is passive for the fluid flow and is assumed to react only with the solid phase in a catalytic manner. As a result, the reactant is converted on the surface of the particle, but no mass and energy is exchanged with the particle. For simplicity, the reaction is further assumed to be neither endothermic nor proceeds at a constant rate λ, which only depends on the surface area of the solid phase. The equation describing the conservation of mass for the isothermal flow is

$$\frac{\mathrm{D}\rho}{\mathrm{D}t} = -\rho\boldsymbol{\nabla}\cdot\boldsymbol{u}, \tag{1}$$

with ρ and $\boldsymbol{u}$ being the fluid density and velocity, respectively, and the advective derivative is given by

$$\frac{\mathrm{D}}{\mathrm{D}t} = \frac{\partial}{\partial t} + \boldsymbol{u}\cdot\nabla. \tag{2}$$

The equation for the conservation of momentum is

$$\rho\frac{\mathrm{D}\boldsymbol{u}}{\mathrm{D}t} = \nabla\cdot(2\mu\boldsymbol{S}) + \rho\boldsymbol{f} + \boldsymbol{F}, \tag{3}$$

where viscous effects are accounted for by the traceless rate of strain tensor $\boldsymbol{S}$ and the dynamic viscosity μ. To obtain statistically stationary isotropic turbulence, we employ a forcing function $\boldsymbol{f}$ equivalent to that of Babkovskaia et al. [1]. The force is acting on the wavevectors lying on a shell in Fourier space with a radius of k_f, accelerating the flow at low wavenumbers. The flow integral scale is given by $L_f = L_x k_1/k_f$ when L_x is the size of the simulation box and $k_1 = 1\ \mathrm{m}^{-1}$ is the wave number of the box size. Since some cases simulated here have significant mass loading, influencing the turbulence field [17, 9], the term $\boldsymbol{F}$ represents the drag force the particle exerts on the fluid phase.

The conservation equation for the molar fraction X of the reactant reads:

$$\frac{\partial X}{\partial t} + \nabla\cdot(X\boldsymbol{u}) = -D\nabla^2 X + \frac{\hat{R}}{\rho}, \tag{4}$$

with D being the diffusivity of the reactant and $\hat{R}$ the source term due to the conversion of the reactant at the particles surface. Thus the reactant can be thought of as oxygen reacting with the carbon of an long lasting char particle without any thermal or flow effects.

2.2. Particle equations

The particles are modeled using a Lagrangian approach. They are spherical and treated as point particles as the particle size is significantly smaller than the grid size. As the density of the particle is magnitudes higher than the fluid phase, we assume that the only force acting on the particle is the Stokes drag. Gravity forces are neglected to achieve a system that is independent of direction. The velocity $\boldsymbol{v}$ of the particle is evolved as

$$\frac{d\boldsymbol{v}}{dt} = \frac{1}{\tau_p}(\boldsymbol{u}-\boldsymbol{v}) = \frac{\boldsymbol{F}}{m_p}, \tag{5}$$

with the particle stopping time given as $\tau_p = Bd_p^2/18\nu(1+f_c)$ when $f_c = 0.15\mathrm{Re}^{0.687}$ is due to the Schiller-Naumann correlation [15]. Here B stands for the density ratio between particle and fluid, d_p is the particles diameter and m_p the particles mass.

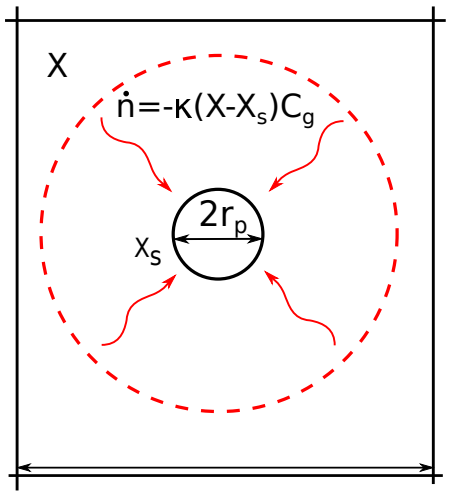

Figure 1: Visualization of the flux to the particles surface

The reactant that is carried by the fluid phase is converted at the particle surface at a rate of $\hat{R} = A_p \dot{n} M / V_{cell}$, where A_p is the particles surface area, $\dot{n}$ is the reactant conversion rate per surface area, M the molar mass of the carrier fluid and V_{cell} the volume of one grid cell. By letting the reactant molar fraction be denoted by X_s at the particles surface and X at a large distance from the surface, one can express the reactant conversion at the surface by $\dot{n} = -\lambda X_s C_g$, where λ is the surface specific molar conversion rate. This is illustrated in Fig. 1. Assuming that the conversion at the surface is in equilibrium with the diffusive flux from the fluid phase to the particles surface $\dot{n} = -\kappa(X - X_s)C_g$, and solving for the surface mole fraction of the reactant, a modified reaction rate $\tilde{\lambda}$ for the reactant conversion is defined as

$$\dot{n} = -\tilde{\lambda} X C_g \tag{6}$$

when $\tilde{\lambda} = \lambda/(1+\lambda C_g/\kappa)$ is obtained following the ideas of Baum and Street [2]. The adapted reaction rate $\tilde{\lambda}$ for the conversion rate will be important when formulating a model for the effect of turbulent clustering on the reactivity. The diffusion coefficient is here given by $\kappa = D\mathrm{Sh}/2r_p$ where the Sherwood coefficient Sh is set to two for all particle sizes representing quiescent flow around the particles for simplicity as the focus in this work is on macroscopic effects.

2.3. The limits of the decay rate

In order to study the effect of turbulent clustering on the reactant conversion it is useful to identify the governing chemical and turbulent time and length scales.

The integral flow time scale $\tau_L = L_f/\boldsymbol{u}_{rms}$ is based on the root mean square of the velocity u_{rms} and the scale of the forcing L_f. It is often claimed that the highest value of the preferential concentration for particles is found for particles with a Stokes number around unity based on the Kolmogorov scale η ([20], [8]). Since for the current study it is the large scale clusters that are interesting, the Stokes number is here, however, defined based on the integral time scale τ_L such that $\mathrm{St} = \tau_p/\tau_L$. Assuming homogeneously distributed particles, the instantaneous value of the reactant molar fraction X is given by:

$$X(t) = X_0 e^{-n_p \tilde{\lambda} A_p t} = X_0 e^{-\alpha_{th} t}. \tag{7}$$

If the initial molar fraction of the reactant X_0 is set to unity, and the particle number density n_p is given, the maximum theoretical decay rate $\alpha_{th} = n_p \tilde{\lambda} A_p$ can thus be estimated. Its inverse $1/\alpha_{th} = \tau_{th}$ is the theoretical reactive time scale.

By defining a Damköhler number $\mathrm{Da} = \tau_L/\tau_{th}$, the evolution of the decay rate α with Damköhler number can be studied. For low particle number densities, and therefore small Damköhler numbers, the macroscopic clustering of particles can be neglected, and $\mathrm{Da} = \tau_L/\tau_{th} = \tau_L \alpha_{th}$ can be formed to yield the *particle* dependent decay rate $\alpha_{th} = \alpha_p = \mathrm{Da}/\tau_L$, which implies that the decay rate increases linearly with the Damköhler number. For higher particle number densities, the macroscopic clusters have high internal particle number densities, which are rapidly converting the reactant within the cluster. Now the decay rate is controlled by the transport of reactant to the surface of these macroscopic clusters, and it is reasonable to consider the particle clusters as single bodies, or super-particles, that the reactants are converted at. One can then formulate a *cluster* dependent decay rate as $\alpha_c = n_c \tilde{\lambda}_c A_c$, which is based on the cluster number density n_c, the modified conversion rate $\tilde{\lambda}_c$ and cluster surface area A_c, which are constants dependent on the macroscopic flow field. One can now estimate values for n_c, $\tilde{\lambda}_c$ and A_c, to find α_c. The following proposed formulation of $\alpha(\mathrm{Da})$ then satisfies the limits as derived at high and low values of Damköhler numbers:

$$\alpha(\mathrm{Da}) = \frac{\alpha_c \mathrm{Da}}{\alpha_c \tau_L + \mathrm{Da}}. \tag{8}$$

This formulation will be compared directly to results from direct numerical simulations in the following section.

3. Results and discussion

The computational domain for the DNS is a cube with an edge length of 2π cm, discretized with 64, 128 or 256 cells which results in grid cell sizes of 981, 490 and 245 μm, respectively with increasing particle numbers. All boundaries are periodic. The strength of the forcing is chosen such that a turbulent Reynolds number $\mathrm{Re} = u_{rms} L_f/\nu$ of approximately 250 is obtained for all cases. Furthermore, the size and density of the particles are chosen to give particle Stokes numbers of St = 0.1 and St = 1.0.

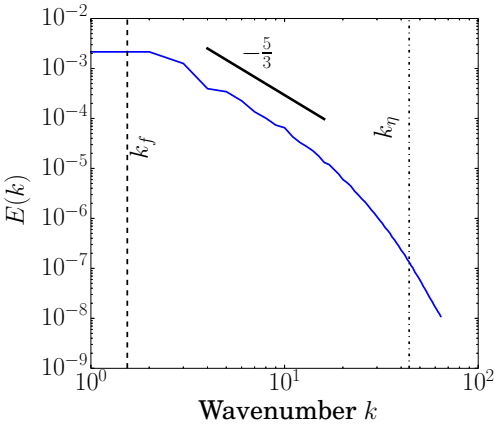

Figure 2: Power spectrum over the wavenumber for a case with a $\mathrm{Re} \approx 250$ and a resolution of 128 cells. Shown are the forcing wavenumber k_f, the wave number of the Kolmogorov scale k_η and the Kolmogorov scaling.

Figure 2 shows the energy spectrum for a case with a Reynolds number of 250. The energy inserted into the domain at the forcing wavenumber k_f (1.5 times

the lowest wavenumber of the domain) is indeed transported to the higher wavenumbers via the inertial subrange, which can be identified by its $-5/3$ slope, before it is dissipated around the Kolmogorov wavenumber k_η.

The simulations are run until the turbulence is statistical stationary, then the molar fraction of the reactant is re-initialized to unity. The decay rate is obtained by fitting an exponential function to the reactant molar fraction from the start of data sampling to later times. The resulting decay rates as function of Damköhler numbers are shown in Fig. 3 for the particle Stokes numbers St = 0.1 and St = 1.0. The deviation of decay rates around the mean are shown by the error bars. The Damköhler number is increased by increasing the number of particles. Furthermore, the proposed modeled decay rate of the reactant molar fraction over the Damköhler number according to Eq. 8 is shown as the solid curve, with the two limiting decay rates α_p and α_c for small and large Damköhler numbers respectively included as dotted and dashed lines. In Fig. 3 it can be seen that for cases with low Damköhler numbers, the decay rate as predicted by DNS is indeed proportional to the Damköhler number and follows clearly α_p, but significant deviations from the linear increase are observed quite early.

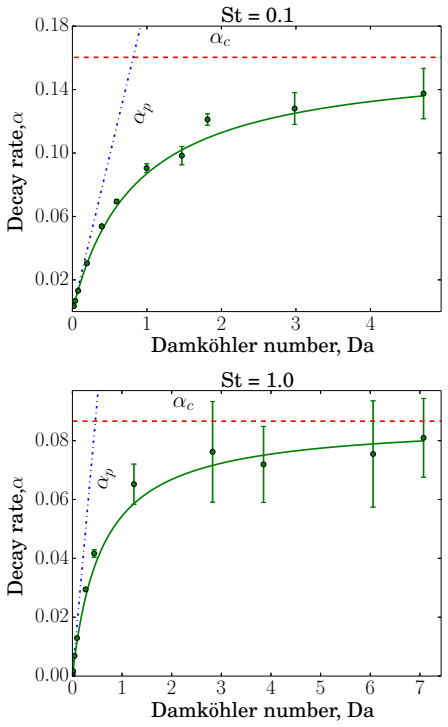

Figure 3: Decay rate over Damköhler number. The upper plots is for $\mathrm{St}_i \approx 0.1$, and the lower for $\mathrm{St}_i \approx 1$. Filler circles represent the decay rates of the numerical simulations, while the solid lines are the fits to the numerical results as given by Eq. 8. The dashed-dotted lines correspond to α_p while the dashed lines represent α_c.

The decay rate begins to deviate from the linear increase (as given by α_p) for Damköhler numbers as small as 0.1. for the given cases. For higher Damköhler numbers the decay rate approaches the flow field dependent decay rate α_c asymptotically. The modeled decay rate α(Da) as defined by Eq. 8 fits the decay given by DNS rather well. Moreover, it is observed that the value of α_c is lower for a higher particle Stokes number. The variance in the decay rates is higher for higher Stokes numbers, and this effect increases in strength for higher Damköhler numbers.

Figure 4 shows a snapshot of the position of every 300th particle (dots) and the upper 90% percentile of the reactant concentration (shaded areas) for particle Stokes numbers St = 0.1 and St = 1.0. For Stokes number of 0.1 the particles tendency to cluster is not visible and the pockets of high reactant concentration are small. Larger areas devoid of particles can be seen at the higher Stokes number, as well as larger volumes of remaining reactant. Overall, the particles in the St = 1.0 runs show stronger large scale clustering than for the St = 0.1 runs.

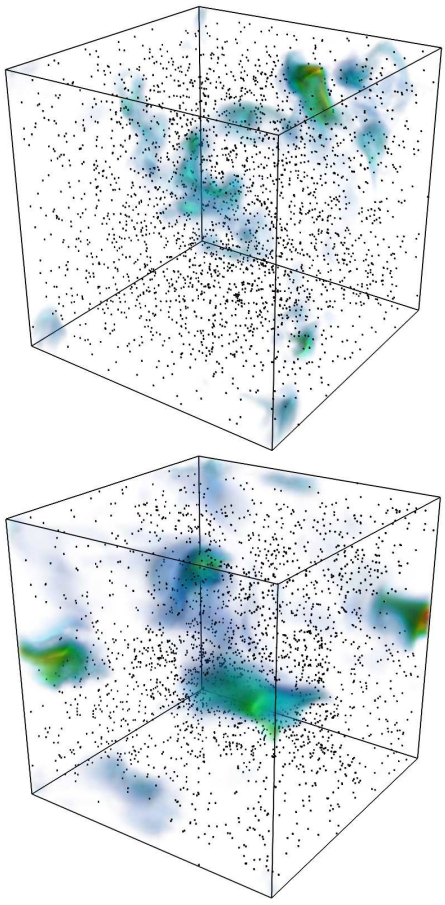

Figure 4: 3D plot of the domain with every 300th particle and the 90th percentile of the reactant concentration.

The probability density, f, for a given reactant

concentration c is shown for two different Damköhler numbers in Fig. 5. The dashed lines represent the probability averaged over the entire domain, while the solid line represent the probability at the position of the particles. For a small Damköhler number of 0.1, it is seen that the distribution is very narrow, and that the probability constraint on the particle position is nearly identical to the probability of all the fluid elements. This means that the reactant concentration is fairly homogeneous, and that it is not affected by the instantaneous position of the particles, i.e. that particle clustering does not influence the reactant distribution in a significant way. For higher Damköhler numbers the distribution is broadening, which means that the reactant distribution is becoming less homogeneous as the importance of the particle clustering is increasing. One can conclude that for large Damköhler numbers the reactions inside the particle clusters are so fast compared to the lifetime of the cluster that the interior of the clusters is essentially always drained of reactants. This means that the reactions are happening at the external surface of the clusters, which resembles how reactants are converted at the external surface of solid objects. This in turn supports the assumption underlying the derivation of the asymptotic limit of α_c.

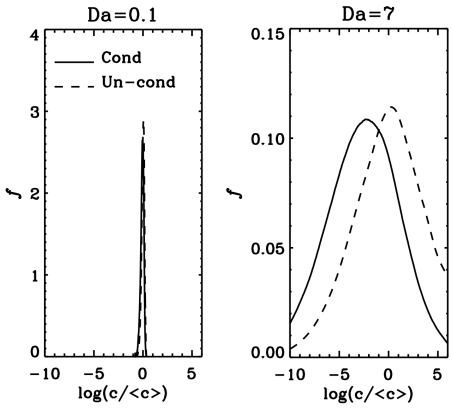

Figure 5: Probability density function of logarithm of the reactant concentration c

The mass loading M_l in the simulations is defined as the ratio of the total mass of the particles $M_p = \sum_i m_{p,i}$ to the total mass of the fluid $M_f = V\overline{\rho}$ such that $M_l = M_p/M_f$. The influence of the mass loading on the turbulent velocities is shown in Fig. 6.

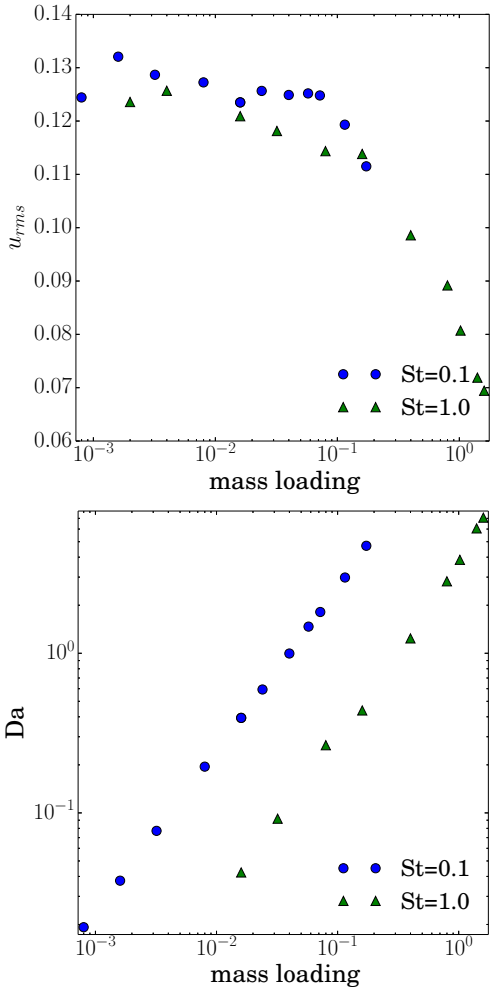

Figure 6: Root mean square of velocity and Damköhler number as function of mass loading $M_l = M_p/M_f$ for two different Stokes numbers.

In the upper panel the turbulent velocity u_{rms} is shown as a function of mass loading. The mass loading does not seem to have any significant effect on the turbulent velocity for low mass loadings, but for larger values of mass loading the turbulent velocity is significantly affected. This change in turbulent intensity will affect the cluster shape and in turn the surface area $\bar{A}_c$. For very high Damköhler numbers, this may reduce the reactivity of the cluster even more than estimated by α_c. In the lower panel of Fig. 6, the Damköhler number is plotted as a function of the mass loading for the two different Stokes numbers. It can be observed that the larger Stokes numbers require higher mass loadings in order to obtain the same Damköhler number.

4. Conclusions

The effect of particle clustering due to flow turbulence on the reaction rate of heterogeneous solid-fluid

reactions is studied in a simplified setup. The particles are assumed to act like catalysts, and a simple one step reaction with the gas phase reactant on the particle surface is assumed to be fast and isothermal. With this simplified setup it is possible to analytically show that for small Damköhler numbers the overall reactivity is found not to be affected by turbulent clustering. However, for large Damköhler numbers, the reaction rates are fast compared to the lifetime of the particle clusters. Hence, the effect of the clusters on the overall reaction rate in the domain becomes important decreasing the overall reaction rate. This effect is stronger for higher Stokes numbers.

A simplified model that gives the reactant decay rate as a function of the turbulent and chemical time scales (see Eq. 8) is proposed. The predictive quantitative abilities of the presented model depend on a good representation of the shape, size and number density of the particle clusters. These aspects of the cluster formation is generally not yet properly understood and further work to understand the shape and number density of particle clusters depending on flow field variables is needed [6]. Furthermore, equivalent investigations using more realistic heterogeneous reaction schemes and fluid phase physics will have to follow.

Acknowledgements

The research leading to these results has received funding from the Polish-Norwegian Research Programme operated by the National Centre for Research and Development under the Norwegian Financial Mechanism 2009-2014 in the frame of Project Contract No Pol-Nor/232738/101/2014. This work was supported by the grant "Bottlenecks for particle growth in turbulent aerosols from the Knut and Alice Wallenberg Foundation, Dnr. KAW 2014.0048 and by grant from Swedish Research Council (Dnr. 638-2013-9243). NELH and DM also acknowledge the Research Council of Norway under the FRINATEK grant 231444.

References

[1] N. Babkovskaia, N.E.L. Haugen, and A. Brandenburg. A high-order public domain code for direct numerical simulations of turbulent combustion. *Journal of Computational Physics*, 230(1):1 – 12, 2011.

[2] M. M. Baum and P. J. Street. Predicting the combustion behaviour of coal particles. *Combustion Science and Technology*, 3(5):231–243, 1971.

[3] Axel Brandenburg. Pencil code homepage, July 2014.

[4] T Brosh and Nilan Chakraborty. Effects of equivalence ratio and turbulent velocity fluctuation on early stages of pulverized coal combustion following localized ignition: A direct numerical simulation analysis. *Energy and Fuels*, 28:6077–0688, 2014.

[5] T. Brosh, D. Patel, D. Wacks, and N. Chakraborty. Numerical investigation of localised forced ignition of pulverised coal particle-laden mixtures: A direct numerical simulation (dns) analysis. *Fuel*, 145:50–62, 2015.

[6] Enrico Calzavarini, Martin Kerscher, Detlef Lohse, and Federico Toschi. Dimensionality and morphology of particle and bubble clusters in turbulent flow. *J. Fluid Mech.*, 607,:pp.13–24,, October 2007.

[7] C Dopazo. *Turbulent reacting flows*. London: Academic Press., 1994.

[8] J. K. Eaton and J. R. Fessler. Preferential concentration of particles by turbulence. *International Journal of Multiphase Flow*, 20:169–209, 1994.

[9] R.A. Gore and C.T. Crowe. Effect of particle size on modulating turbulent intensity. *International Journal of Multiphase Flow*, 15(2):279 – 285, 1989.

[10] W.P Jones and B.E Launder. The prediction of laminarization with a two-equation model of turbulence. *International Journal of Heat and Mass Transfer*, 15(2):301 – 314, 1972.

[11] A. Yu. Klimenko and R.W. Bilger. Conditional moment closure for turbulent combustion. *Progr. Energy Combustion Sci.*, 25:595–687, 1999.

[12] Kun Luo, Haiou Wang, Jianren Fan, and Fuxing Yi. Direct Numerical Simulation of Pulverized Coal Combustion in a Hot Vitiated Co-flow. *Energy & Fuels*, 26(10):6128–6136, OCT 2012.

[13] Bjørn Magnussen and Bjørn Hjertager. On mathematical models of turbulent combustion with special emphasis on soot formation and combustion. *Proceedings of the Combustion Institute*, 16(1):719729, 1979.

[14] Stephen B. Pope. *Turbulent Flows*. Cambridge University Press, 2000.

[15] Schiller and Naumann. über die grundlegenden berechnungen bei der schwerkraftaufbereitung. *Verein Deutscher Ingenieure*, 77:318, 1933.

[16] Armin Silaen and Ting Wang. Effect of turbulence and devolatilization models on coal gasification simulation in an entrained-flow gasifier. *International Journal of Heat and Mass Transfer*, 53(9-10):2074–2091, APR 2010.

[17] K. D. Squires and J. K. Eaton. Particle response and turbulence modification in isotropic turbulence. *Physics of Fluids*, 7:1191–12–3, 1990.

[18] Michele Vascellari, Daniel G. Roberts, San Shwe Hla, David J. Harris, and Christian Hasse. From laboratory-scale experiments to industrial-scale CFD simulations of entrained flow coal gasification. *Fuel*, 152:58 – 73, 2015.

[19] J.H Williamson. Low-storage runge-kutta schemes. *Journal of Computational Physics*, 35(1):48 – 56, 1980.

[20] A. M. Wood, W. Hwang, and J. K. Eaton. Preferential concentration of particles in homogeneous and isotropic turbulence. *International Journal of Multiphase Flow*, 31:1220–1230, 2005.